Published in final edited form as:
Photochem Photobiol. 2012 September ; 88(5): 1191–1197. doi:10.1111/j.1751-1097.2011.01038.x.

The Role of Cholesterol In Ultraviolet Light B-Induced Apoptosis†

Kimberly S. George[a,b,d], **Walid Elyassaki**[a,c,d], **Qiong Wu**[a], and **Shiyong Wu**[a,*]

[a]Edison Biotechnology Institute and Department of Chemistry and Biochemistry, Ohio University, Athens, Ohio 45701, USA

[b]Department of Chemistry, Marietta College, Marietta, OH 45750, USA

[c]Battelle Memorial Institute, Charlottesville, VA 22902, USA

Abstract

Modification of major lipid raft components, such as cholesterol and ceramide, plays a role in regulation of programmed cell death under various stimuli. However, the relationship between cholesterol level modification and the activation of apoptotic signaling cascades upon ultraviolet B light has not been established. In this report, we demonstrate that upon UVB irradiation cholesterol levels in membrane rafts of skin cells increase, which leads to Fas aggregation in the rafts. Utilizing a continuous velocity floatation technique, we show that Fas accumulated in the lipid rafts of human melanoma M624 cells after UVB-irradiation. The subsequent events of DISC formation were also detected in the lipid raft fractions. Depletion of cholesterol by methyl-β-cyclodextrin reduces Fas aggregation, while overloading increases. Disruption of lipid rafts also prevents Daxx from dissociating from Fas in the lipid rafts, which is accompanied with a reduced apoptotic, but increased non-apoptotic death of UVB-irradiated human keratinocytes, HaCaT cells. Results indicate that cholesterol located in the plasma membrane of skin cells is required for lipid raft domain formation and activation of UVB-induced apoptosis.

INTRODUCTION

Lipid rafts are heterogeneous in both protein and lipid content, and different types of lipid rafts coexist within a cell membrane (1–3). The structure of lipid rafts is dynamic, resulting in an ever-changing content of both lipids and proteins. The major components of lipid rafts are cholesterol, sphingolipids, and caveolins. Lipid rafts play an important role in regulation of many signaling pathways including but not limited to apoptosis (4–10), cell-cell interaction (11–15), and immune responses (16–19). Treating cells with cholesterol-depleting agent methyl-β-cyclodextrin (MβCD) removes cholesterol from the lipid rafts and leads to conformational changes in the raft structure that consequently affect the death receptors located on the membrane (20–24). In accordance with “The Induced-Fit Model of Raft Heterogeneity”, the association of proteins with lipid rafts can affect the lipid content of the lipid rafts and vice versa (1,25). Lipid raft microdomains provide signaling platforms capable of activating various cellular signaling pathways, both pro-apoptotic and anti-apoptotic, which may be inhibited upon lipid raft disruption (8,26,27).

†This paper is part of the Special Issue in Commemoration of the 70th birthday of Dr. David R. Bickers

*Corresponding author: Dr. Shiyong Wu (wus1@ohio.edu), Phone:(740) 597-1318, Fax:(740) 593-4795.
[d]The authors have equal contribution.

Fas receptor (Fas, Apo-1 or CD95) aggregation and the death-inducing signaling complex (DISC) formation play a critical role in regulation of apoptosis upon ultraviolet light (UV) irradiation (20,21,28,29). We have previously shown that lipid rafts mediate UVB-induced apoptosis through recruiting and promoting Fas aggregation, DISC formation and Fas-FADD (Fas-associated death domain protein)-caspase 8 cascade activation in human melanoma cell line M624 (22). Ultraviolet (UV) irradiation alters cholesterol levels in skin epidermal cells (23,24) and in lipid rafts of cultured cells (22). However, the effect of cholesterol alternation on apoptosis upon ultraviolet B (UVB) irradiation is not clear. In this report, we provide evidence that cholesterol levels in cells are increased and then decreased after UVB-irradiation. The elevation of cholesterol in the cells and lipid rafts of the cells in the early time after the irradiation leads to Fas aggregation and cell apoptosis. Disruption of lipid rafts by cholesterol depletion protects cells from UVB-induced apoptosis. However, depending on the cell type, cholesterol depletion could also promote non-apoptotic death of the cells with or without being UVB-irradiated.

MATERIALS AND METHODS

Cell culture

Human keratinocytes HaCaT cells were maintained in DMEM supplemented with 10% fetal bovine serum (FBS) and 1% penicillin/streptomycin at 37°C and with 5% carbon dioxide (CO_2). Human melanoma M624 cells were maintained in DMEM containing 10% FBS at 37°C with 5% CO_2. Cells were seeded 12 hours prior to treatment.

UVB irradiation

Cells were irradiated with UVB (290–320 nm) generated by a 15 W UVB light source (UVBP Inc). The intensity of UVB light was measured using a UVB-meter (UVBP Inc.). The cells were irradiated with 50 mJ/cm^2 of UVB light. The culture medium was replaced with PBS during exposure.

Cholesterol level alteration and Caspase inhibition

Rapid depletion of cholesterol was achieved by culturing the cells in serum free medium containing 10 mM MβCD (Sigma-Aldrich) at 37°C for one hour prior to UVB irradiation. The cells were then cultured in reduced serum medium containing 1% FBS with 1 mM MβCD at 37°C until harvesting.

Addition and incorporation of cholesterol into the cell membrane was achieved through incubation of cells in medium containing 50 μg/mL exogenous cholesterol (Sigma-Aldrich) at 37°C for 1 h prior to UVB irradiation. The cells were then cultured in medium containing 5 μg/mL exogenous cholesterol at 37°C until harvesting.

The broad caspase inhibitor Q-VD-Oph (10 μM) was add to the cells 2 h before UVB treatment and kept in the culture medium until harvest.

Isolation of lipid rafts using Optiprep™ gradient

Lipid rafts of HaCaT cells were isolated according to a recently improved procedure (30). Briefly, cells were washed with cold PBS, treated with 3,3'-dithiobis [sulfosuccinimidylpropionate] (DTSSP) (Thermo Scientific Pierce) at 1.25 mM for 1 h on ice, scraped from plates in cold PBS containing 5 mM Ethylenediaminetetraacetic acid (EDTA) and centrifuged at 10,000 rpm for ten minutes. The cell pellet was frozen at −80°C overnight, washed with cold PBS, and homogenized in TNET buffer (50 mM Tris-HCl pH 7.4, 150 mM NaCl, 5 mM EDTA, 0.1% Triton X-100) by forcing cells through a 23-gauge needle. Cell lysates were combined with OptiPrep™ (Axis Shield) separation medium and

placed at the bottom of a 40-30-5% iodixanol step gradient. Gradients were placed in a SW60 swing bucket rotor tube (Beckman-Coulter) and ultracentrifuged at 4°C at 31,300 rpm for five hours. A portion of each whole cell lysate was saved for analysis. Five fractions of equal volume were retrieved from the tube after ultracentrifugation.

Lipid rafts of M624 cells were isolated according to our previous procedure (22). Briefly, the cells were washed with cold PBS and scraped from plates in TNET buffer. After homogenizing the cells using a sonicator, the homogenates were adjusted to 30% in Optiprep™ and placed at the bottom of a continuous gradient. The gradient was centrifuged at 35,000 rpm overnight in an SW60 rotor (Beckman-Coulter). Six equal fractions were collected and the cell debris at the bottom of the gradient was discarded.

Immunoblotting

Equal volumes/protein amounts of sample fractions and whole cell lysates were buffered and SDS-PAGE was performed followed by semi-dry transfer to nitrocellulose membrane. Membranes were blocked with dry milk and then probed with primary antibodies specific to the following proteins followed by corresponding secondary antibodies: caveolin-1 (n-20, sc-894), Daxx, (M-112, sc-7152), FADD (S-18, sc-6035) and Fas (C-20, sc-715) from Santa Cruz Biotechnology, PARP (9542) from Cell Signaling, and β-actin (A5316) from Sigma Aldrich.

Cholesterol and protein analysis

The Wako Cholesterol E kit (Wako Chemicals), an enzymatic colorimetric method for the quantitative determination of total cholesterol in samples, was used as per manufacturer's instructions. The Bradford Protein Assay Kit (Bio-Rad Laboratories) was used as per manufacturer's instructions. The absorbances of the solutions from the cholesterol and protein assays were measured at 600 nm and 595 nm, respectively.

Clonogenic assays

Cells (5×10^3) were seeded in a 60 mm culture plate and allowed to adhere overnight prior to treatment. At 7 days after treatment, the cells were washed with PBS twice and fixed by cold methanol for 10 min at −20°C. The fixed cells were stained by 0.5% (w/v) crystal violet in 25% methanol for 10 min at room temperature.

Viability Assay

Viability of M624 cells was determined using Alamar Blue, a metabolic activity assay. Cells (5×10^4 cells) in 1 mL media were seeded in each well of 24-well plates and allowed to adhere overnight before UVB-irradiation. At 48 h post-UVB treatment, 100 μL Alamar Blue (Biosource) was added to each well and the cells were incubated for three more hours as per assay instructions. Absorbance was then read at 570 and 600 nm on a Spectramax M2 plate reader (Molecular Devices) and percent change in metabolic activity was calculated using the equation: $[(\Sigma_{ox})_{600} \times A_{570} - (\Sigma_{ox})_{570} \times A_{600}$ of test agent]/ $[(\Sigma_{ox})_{600} \times A_{570} - (\Sigma_{ox})_{570} \times A_{600}$ of positive growth control] × 100, where $(\Sigma_{ox})_{600} = 117{,}216$ and $(\Sigma_{ox})_{570} = 80{,}586$.

Caspase 3 activity assay

Caspase 3 activity was determined by using a fluorometric assay method. Briefly, 25 μg of the cytosolic extract was initially diluted to a volume of 100 μL with caspase assay buffer (10 mM HEPES, pH 7.4, 2 mM EDTA, 0.1% CHAPS, 5mM DTT). The aliquots were mixed with an equal amount (100 μL) of 40 μM fluorescent tetrapeptide substrate specific for caspase 3 (Ac-DEVD-AMC, Bachem Bioscience) in caspase assay buffer and transferred to 96-well plates. Free aminomethylcoumarin (AMC), generated as a result of cleavage of

the aspartate-AMC bond, was monitored with a Spectra-max M2 Fluorescence plate reader (Molecular Devices Corp) at excitation and emission wavelengths of 360 nm and 460 nm, respectively.

Ceramide analysis

Ceramide was detected using the dot-blot method. Briefly, samples were blotted onto a nitrocellulose membrane which was then blocked with dry milk. The membrane was incubated with anti-ceramide antibody (MID 15B4, Alexis Biochemicals) and corresponding secondary antibody.

Lipid raft fluorescent labeling

Lipid rafts were labeled with Alexa Fluor 488-conjugated anti-GM1 (Invitrogen), which is known to be specifically associated with the lipid rafts. Labeling was performed for 1 h following 50 mJ/cm^2 UVB irradiation. Cells were visualized using a confocal microscope (LSM 510, Carl Zeiss) at excitation and emission wavelengths of 495 nm and 519 nm, respectively.

RESULTS

Cholesterol-dependent Fas aggregation in lipid rafts of M624 melanoma cells after UVB-irradiation

Our previous study demonstrated that an increased Fas aggregation in lipid rafts and apoptosis after UVB-irradiation was correlated to a reduced level of total cholesterol and rafts' cholesterol in M624 melanoma cells (22). To determine the role of the raft cholesterol in regulation of UVB-induced Fas aggregation and cell apoptosis, we analyzed the extent of the effect of cholesterol addition or depletion on lipid raft association of Fas and FADD. As we previously showed, Fas and FADD was present in increased levels in the lipid raft fractions 2–5 after UVB irradiation (Fig. 1, +UVB vs. Control). This translocation of Fas and FADD into lipid raft domains following UVB irradiation was inhibited by the disruption of lipid raft domains caused by cholesterol depletion (Fig. 1, −Chol/+UVB vs. +UVB). Addition of exogenous cholesterol to cells prior to UVB irradiation had little to no effect on the recruitment of FADD to the lipid rafts of M624 cells (Fig. 1, +Chol/+UVB vs. Control). These results indicate that the aggregation and activation of Fas, as well as the recruitment of FADD to the lipid rafts are cholesterol-dependent, but not likely due to the UVB-induced reduction of cholesterol in M624 melanoma cells as we previously predicted.

Role of cholesterol in UVB-induced apoptosis of M624 melanoma cells

To further characterize the role of cholesterol in regulation of UVB-induced apoptosis, we determined the extent of the effect of a broad caspase inhibitor Q-VD-OPH on viability of M624 cells after the treatment. Our data shows that depletion or overload of cholesterol slightly reduced cell viability by 10.8±5.5% and 14.7±4.9%, respectively, at 48 h post treatment (Fig. 2A). UVB alone reduced cell viability by 53.3±2.6%. A combination of cholesterol depletion and UVB reduced cell viability by only 36.9±3.5% (Fig. 2A). In contrast, a combination of cholesterol overload and UVB reduced cell viability by 65.0±2.0% (Fig. 2A). Interestingly, Q-VD-OPH treatment increased cell viabilities by 25.0% (78.3±5.1%−53.3±2.6%) and 22.7% (59.6±3.8%−36.9±3.5%) for UVB alone and a combination of cholesterol overload and UVB, respectively (Fig. 2A). However, Q-VD-OPH treatment has almost no effect on viability of cells treated with a combination of MβCD and UVB (Fig. 2A). These results suggest that cholesterol depletion protects the cells from UVB-induced apoptosis, while cholesterol overload could be additive to the effect of UVB in induction of apoptosis.

To confirm the role of cholesterol in mediating apoptotic signaling in melanoma cells after UVB irradiation, we examined caspase 3 activity after the treatment. An elevation of caspase 3 activity is correlated to a reduced viability of the cells after each treatment (Fig. 2B vs. 2A). These results further demonstrate that cholesterol plays a critical role in regulation of apoptotic death of M624 melanoma cells after UVB irradiation.

Alternation of cholesterol levels in M624 cells after UVB irradiation

To determine the potential mechanism for UVB-induced and cholesterol-dependent Fas aggregation, we analyzed total cholesterol concentration in whole cell lysate prepared from cells treated with or without MβCD or exogenous cholesterol in the presence or absence of UVB-irradiation. Our data showed that the cholesterol level was increased in cells up to 26% from 1 to 3 h before it was decreased up to 52% from 6 to 48 h post-UVB (Fig. 3). MβCD treatment reduced the cholesterol level in the cells by 16–25% and prevented an UVB-induced elevation of cholesterol at 3 h post irradiation (Fig. 3). Overload of cholesterol increased the cholesterol level in the cells by 70% and by 120% at 3 h post irradiation (Fig. 3). These results suggest that while an increase of cholesterol alone has limited effects on cell death, a combination of increased cholesterol and UVB is required for the induction of cell death in M624 cells, since depletion of cholesterol reduced UVB-induced cell death.

The effect of cholesterol depletion on survival and apoptosis of HaCaT keratinocytes after UVB irradiation

To determine whether cholesterol plays a similar role in UVB-induced apoptosis of keratinocytes, we analyzed the translocation and activation of Fas in lipid rafts of HaCaT cells after UVB and/or MβCD treatment. Using a recently improved method of lipid raft isolation (30), we demonstrate that caveolin-1 is located exclusively in fraction 2 of the HaCaT cell lipid raft isolation in all treatment groups, indicating that the lipid rafts of the cells are exclusively located in this fraction (Fig. 4A). Our data showed that Fas almost exclusively existed in the lipid raft fraction and there was no significant translocation of Fas detected after UVB-irradiation (Fig. 4A). However, the treatment of MβCD promoted translocation of Fas from the inside of lipid raft domains (Fraction 2) to the outside of the lipid rafts (Fraction 4) (Fig. 4A). In order to determine the correlation between raft association of Fas and DISC formation, we analyzed Fas-binding proteins FADD and Daxx in the gradient fractions. While FADD was undetectable in all fractions (data not shown), lipid raft-associated Daxx was reduced after UVB-irradiation (Fig. 4A) and MβCD treatment prevented the reduction of Daxx in the raft fraction (Fig. 4A). These results suggest that UVB might induce a reorganization of lipid rafts and that cholesterol plays a role in regulation of the association of Fas-binding protein(s) with the lipid rafts in HaCaT cells.

To determine the effect of cholesterol depletion on UVB-induced cell death of keratinocytes, clonogenic assays were performed on HaCaT cells receiving UVB and/or MβCD treatment. A reduced colony formation was observed following either of the treatments alone, as well as in combination (Fig. 4B). In contrast to its mild effect on melanoma viability and its protective effect on UVB-induced melanoma apoptosis, MβCD demonstrated a highly toxic effect in HaCaT cells and further reduced the survival rate of UVB-irradiated cells (Fig. 4B). In order to differentiate between apoptotic and necrotic cell death, analysis of the cleavage of the protein poly-(ADP-ribose) polymerase (PARP) was performed following cell treatment. Our data indicated that MβCD alone reduced cell viability without increasing PARP cleavage (Fig. 4C, Lane 3 vs. 1). However, PARP cleavage and total PARP in cells that were treated with both MβCD and UVB were significantly less than that in cells only treated with UVB (Fig. 4C, Lane 4 vs. 2). These results indicate that depletion of cholesterol

is able to induce non-apoptotic death of keratinocytes and to shift UVB induced apoptosis to necrosis in HaCaT cells.

Alternation of chemical and physical behavior of lipid rafts in HaCaT cells after UVB

To determine the effect of UVB on major lipid components in the rafts of keratinocytes, cholesterol and ceramide levels were monitored before and after UVB-irradiation. Upon receiving UVB, levels of cholesterol in fraction 2 were elevated, while levels of cholesterol located elsewhere in the cell/on the gradient remained relatively constant (Fig. 5A). The amount of ceramide present in fraction 2 decreased following UVB, while the amount of ceramide present in fraction 4 of the isolation procedure slightly increased (Fig. 5B). These results indicate that while cholesterol was integrated into raft domains, ceramide translocates from the inside to the outside of raft domains on the membrane upon irradiation. These results also suggest that cholesterol and ceramide, present as main components of lipid raft domains, might compensate for one another in rafts.

To determine whether the alternation of chemical components in raft domains impact the physical behavior of lipid rafts of HaCaT cells upon UVB irradiation, lipid rafts of cells were fluorescently labeled and visualized using confocal microscopy before and after UVB irradiation. Lipid rafts of UVB-irradiated HaCaT cells were thinner and smaller than those of non-irradiated cells, and they formed clusters along the cell membrane. No clusters were present in the larger, thicker lipid rafts present in the non-irradiated cells (Fig. 5C).

DISCUSSION

UV irradiation induces Fas aggregation and DISC formation (FAS, FADD, Caspase 8), which is essential for UV-induced apoptosis (20,21,28,29). Our previous studies demonstrated that lipid rafts play a critical role in Fas aggregation and DISC formation in M624 melanoma cells upon UVB-irradiation (22). We also demonstrated that an increased Fas aggregation in lipid rafts and apoptosis after UVB irradiation was correlated to a reduced level of total cholesterol and rafts' cholesterol in M624 melanoma cells (22). The role of cholesterol and lipid rafts in promoting cell death was previously discussed (6,31). Depending on the stimulation and apoptotic factors involved, disruption of lipid rafts integrity can be pro- or anti-apoptotic (8,26,27,32). In this study, we determine the role of cholesterol in UVB-induced apoptosis of melanoma cells and keratinocytes. Our data indicate that increased cholesterol levels occurring 1–3 hours after UVB irradiation (Fig. 3) might be responsible for Fas aggregation and DISC formation in lipid rafts since cholesterol depletion by MβCD prevented the translocation of Fas and FADD into raft domains of M624 cells after UVB irradiation (Fig. 1). The involvement of cholesterol elevation in UVB-induced apoptosis of melanoma cells was further demonstrated. UVB-induced caspase 3 activation and apoptosis in M624 cells and M624 cells treated with exogenous cholesterol can be partially prevented by treating the cells with MβCD or a broad caspases inhibitor Q-VD-Oph (Fig. 2). However, the caspase inhibitor has almost no effect on cell viability and caspase 3 activity of the M624 cells treated with a combination of MβCD and UVB (Fig. 2), indicating that these cells are not undergoing apoptotic death.

In HaCaT cells, Fas almost exclusively exists in the lipid rafts with or without UVB irradiation. It appears that Fas are aggregated and activated within the lipid rafts without translocation into the rafts in HaCaT cells after UVB irradiation. The Fas aggregation was monitored by analyzing the association of Fas binding proteins FADD and Daxx. Unfortunately, FADD was present in such a low concentration in HaCaT cells that it was undetectable in the gradient fractions using conventional western blotting methods, so we were unable to verify the initiation of this apoptotic pathway. However, previous studies indicate the initiation of this apoptotic caspase cascade in HaCaT cells upon UV irradiation

(21). The presence of Daxx in lipid rafts was observed (Fig. 4A). Interestingly, lipid raft-associated Daxx was reduced after UVB-irradiation, which implies that UVB-induced recruitment of FADD competes with Daxx in binding to Fas as we previously suggested (33). Disruption of lipid rafts and Fas aggregation by MβCD restored the presence of Daxx in lipid rafts (Fig. 4A). In addition, an elevation of cholesterol and a reduction of ceramide in lipid rafts (Fig. 5A–B) accompanied by raft morphological changes (Fig. 6) after UVB irradiation was correlated to reduced cell viability (Fig. 4B) and increased PARP cleavage (Fig. 4C), indicating the apoptotic death of the HaCaT cells. Disruption of lipid rafts by MβCD reduced raft-associated Fas and PARP cleavage, but promoted cell death with or without UVB-irradiation (Fig. 4A–C), suggesting that lipid raft disruption led to a non-apoptotic death of HaCaT cells.

In summary, we conclude from the presented data that alterations in lipid content, especially the elevation of cholesterol caused by UVB irradiation leads to aggregation and activation of apoptotic signaling pathways, such as the Fas-FADD cascade in cells. Depending on the cell type, a disruption of lipid rafts by MβCD could protect cells from UVB-induced apoptosis, but might also promote non-apoptotic death of the treated cells.

Acknowledgments

This work was partially supported by NIH RO1CA086928 (to S. Wu), Graduate Assistantship (to K.S. George) from BMIT and the Department of Chemistry and Biochemistry, Ohio University and Graduate Research Enhancement Award (to K.S. George) from the College of Arts and Science at Ohio University.

ABBREVIATIONS

UVB	ultraviolet light (290–320 nm)
Fas	Fas-receptor
FADD	Fas-associated death domain
PARP	nuclear enzyme poly (ADP-ribose) polymerase
MβCD	methyl-β-cyclodextrin
Daxx	Fas death domain-associated protein

REFERENCES

1. Pike LJ. Lipid rafts: heterogeneity on the high seas. Biochem J. 2004; 378:281–292. [PubMed: 14662007]
2. Pike LJ. Growth factor receptors, lipid rafts and caveolae: an evolving story. Biochim Biophys Acta. 2005; 1746:260–273. [PubMed: 15951036]
3. Brown DA, London E. Functions of lipid rafts in biological membranes. Annu Rev Cell Dev Biol. 1998; 14:111–136. [PubMed: 9891780]
4. Cottin V, Doan JE, Riches DW. Restricted localization of the TNF receptor CD120a to lipid rafts: a novel role for the death domain. J Immunol. 2002; 168:4095–4102. [PubMed: 11937569]
5. Deans JP, Li H, Polyak MJ. CD20-mediated apoptosis: signalling through lipid rafts. Immunology. 2002; 107:176–182. [PubMed: 12383196]
6. Scheel-Toellner D, Wang K, Singh R, Majeed S, Raza K, Curnow SJ, Salmon M, Lord JM. The death-inducing signalling complex is recruited to lipid rafts in Fas-induced apoptosis. Biochem Biophys Res Commun. 2002; 297:876–879. [PubMed: 12359234]
7. Muppidi JR, Siegel RM. Ligand-independent redistribution of Fas (CD95) into lipid rafts mediates clonotypic T cell death. Nat Immunol. 2004; 5:182–189. [PubMed: 14745445]

8. Bang B, Gniadecki R, Gajkowska B. Disruption of lipid rafts causes apoptotic cell death in HaCaT keratinocytes. Exp Dermatol. 2005; 14:266–272. [PubMed: 15810884]
9. zum Buschenfelde CM, Wagner M, Lutzny G, Oelsner M, Feuerstacke Y, Decker T, Bogner C, Peschel C, Ringshausen I. Recruitment of PKC-betall to lipid rafts mediates apoptosis-resistance in chronic lymphocytic leukemia expressing ZAP-70. Leukemia : official journal of the Leukemia Society of America, Leukemia Research Fund, U.K. 2010; 24:141–152.
10. Xiao W, Ishdorj G, Sun J, Johnston JB, Gibson SB. Death receptor 4 is preferentially recruited to lipid rafts in chronic lymphocytic leukemia cells contributing to tumor necrosis related apoptosis inducing ligand-induced synergistic apoptotic responses. Leukemia & lymphoma. 2011; 52:1290–1301. [PubMed: 21699383]
11. Del Pozo MA. Integrin signaling and lipid rafts. Cell Cycle. 2004; 3:725–728. [PubMed: 15197344]
12. Singleton PA, Bourguignon LY. CD44 interaction with ankyrin and IP3 receptor in lipid rafts promotes hyaluronan-mediated Ca2+ signaling leading to nitric oxide production and endothelial cell adhesion and proliferation. Exp Cell Res. 2004; 295:102–118. [PubMed: 15051494]
13. Yanagisawa M, Nakamura K, Taga T. Roles of lipid rafts in integrin-dependent adhesion and gp130 signalling pathway in mouse embryonic neural precursor cells. Genes Cells. 2004; 9:801–809. [PubMed: 15330857]
14. Tsuda K, Furuta N, Inaba H, Kawai S, Hanada K, Yoshimori T, Amano A. Functional analysis of alpha5beta1 integrin and lipid rafts in invasion of epithelial cells by Porphyromonas gingivalis using fluorescent beads coated with bacterial membrane vesicles. Cell Struct Funct. 2008; 33:123–132. [PubMed: 18388398]
15. Vassilieva EV, Gerner-Smidt K, Ivanov AI, Nusrat A. Lipid rafts mediate internalization of beta1-integrin in migrating intestinal epithelial cells. Am J Physiol Gastrointest Liver Physiol. 2008; 295:G965–G976. [PubMed: 18755811]
16. Setterblad N, Becart S, Charron D, Mooney N. B cell lipid rafts regulate both peptide-dependent and peptide-independent APC-T cell interaction. Journal of immunology. 2004; 173:1876–1886.
17. Sigal LH. Molecular biology and immunology for clinicians 29: lipid domains, lipid rafts, and caveolae. Journal of clinical rheumatology : practical reports on rheumatic & musculoskeletal diseases. 2004; 10:143–146.
18. Larbi A, Dupuis G, Khalil A, Douziech N, Fortin C, Fulop T Jr. Differential role of lipid rafts in the functions of CD4+ and CD8+ human T lymphocytes with aging. Cellular signalling. 2006; 18:1017–1030. [PubMed: 16236485]
19. Cho JH, Kim HO, Surh CD, Sprent J. T cell receptor-dependent regulation of lipid rafts controls naive CD8+ T cell homeostasis. Immunity. 2010; 32:214–226. [PubMed: 20137986]
20. Rehemtulla A, Hamilton CA, Chinnaiyan AM, Dixit VM. Ultraviolet radiation-induced apoptosis is mediated by activation of CD- 95 (Fas/APO-1). J Biol Chem. 1997; 272:25783–25786. [PubMed: 9325306]
21. Aragane Y, Kulms D, Metze D, Wilkes G, Poppelmann B, Luger TA, Schwarz T. Ultraviolet light induces apoptosis via direct activation of CD95 (Fas/APO-1) independently of its ligand CD95L. J Cell Biol. 1998; 140:171–182. [PubMed: 9425165]
22. Elyassaki W, Wu S. Lipid rafts mediate ultraviolet light-induced Fas aggregation in M624 melanoma cells. Photochem Photobiol. 2006; 82:787–792. [PubMed: 16438619]
23. Datsenko ZM, Semenov VL, Bendt VP. Effects of UV-radiation of different spectral composition on content of sterols in rat skin. Ukr Biokhim Zh. 1976; 48:86–88. [PubMed: 1258165]
24. Picardo M, Zompetta C, De Luca C, Cirone M, Faggioni A, Nazzaro-Porro M, Passi S, Prota G. Role of skin surface lipids in UV-induced epidermal cell changes. Arch Dermatol Res. 1991; 283:191–197. [PubMed: 1867482]
25. Abrami L, Fivaz M, Kobayashi T, Kinoshita T, Parton RG, van der Goot FG. Cross-talk between caveolae and glycosylphosphatidylinositol-rich domains. J Biol Chem. 2001; 276:30729–30736. [PubMed: 11406621]
26. Algeciras-Schimnich A, Shen L, Barnhart BC, Murmann AE, Burkhardt JK, Peter ME. Molecular ordering of the initial signaling events of CD95. Mol Cell Biol. 2002; 22:207–220. [PubMed: 11739735]

27. Li HY, Appelbaum FR, Willman CL, Zager RA, Banker DE. Cholesterol-modulating agents kill acute myeloid leukemia cells and sensitize them to therapeutics by blocking adaptive cholesterol responses. Blood. 2003; 101:3628–3634. [PubMed: 12506040]

28. Leverkus M, Yaar M, Gilchrest BA. Fas/Fas ligand interaction contributes to UV-induced apoptosis in human keratinocytes. Exp Cell Res. 1997; 232:255–262. [PubMed: 9168800]

29. Caricchio R, Reap EA, Cohen PL. Fas/Fas ligand interactions are involved in ultraviolet-B-induced human lymphocyte apoptosis. J Immunol. 1998; 161:241–251. [PubMed: 9647230]

30. George KS, Wu Q, Wu S. Effects of freezing and protein cross-linker on isolating membrane raft-associated proteins. Biotechniques. 2010; 49:837–838. [PubMed: 21091450]

31. Ryan L, O'Callaghan YC, O'Brien NM. Generation of an oxidative stress precedes caspase activation during 7beta-hydroxycholesterol-induced apoptosis in U937 cells. J Biochem Mol Toxicol. 2004; 18:50–59. [PubMed: 14994280]

32. Mu Y, Lv S, Ren X, Jin G, Liu J, Yan G, Li W, Shen J, Luo G. UV-B induced keratinocyte apoptosis is blocked by 2-selenium-bridged beta-cyclodextrin, a GPX mimic. J Photochem Photobiol B. 2003; 69:7–12. [PubMed: 12547491]

33. Wu S, Loke HN, Rehemtulla A. Ultraviolet radiation-induced apoptosis is mediated by Daxx. Neoplasia. 2002; 4:486–492. [PubMed: 12407442]

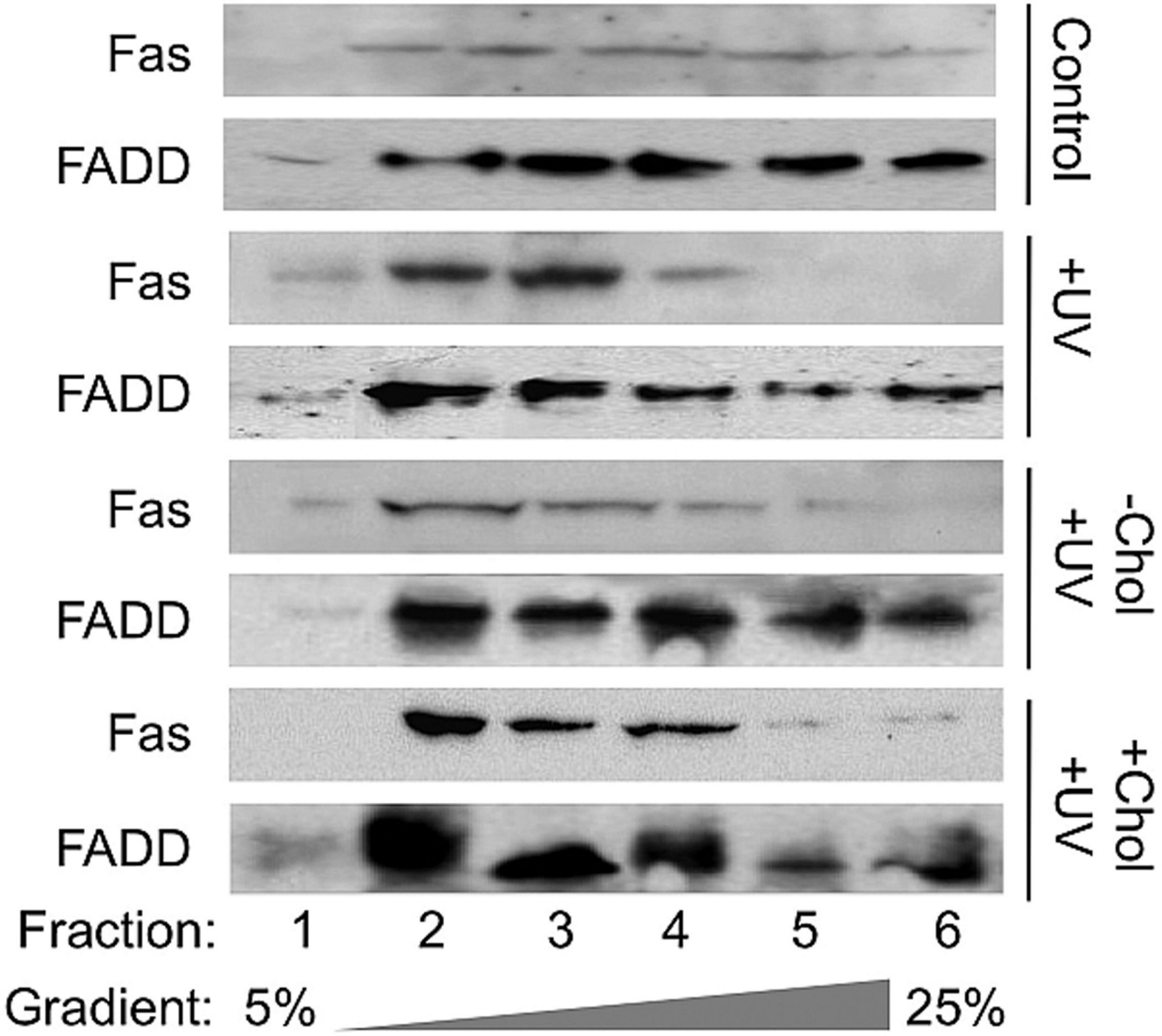

Figure 1.

Fas and FADD distributions in gradient fractions of UVB-irradiated, cholesterol-depleted and cholesterol-enriched M624 cells. Total cell lysates were prepared from UVB-irradiated, cholesterol-depleted and cholesterol-enriched M624 cells and fractionated on an Optiprep continuous gradient (25-5%). Equal volumes of each gradient fraction was buffered and SDS-PAGE was performed. Proteins were electroblotted onto nitrocellulose membrane, the membrane was blocked, and the distributions of Fas and FADD were analyzed by immunoblot using the corresponding antibodies. Results are representative of three independent experiments.

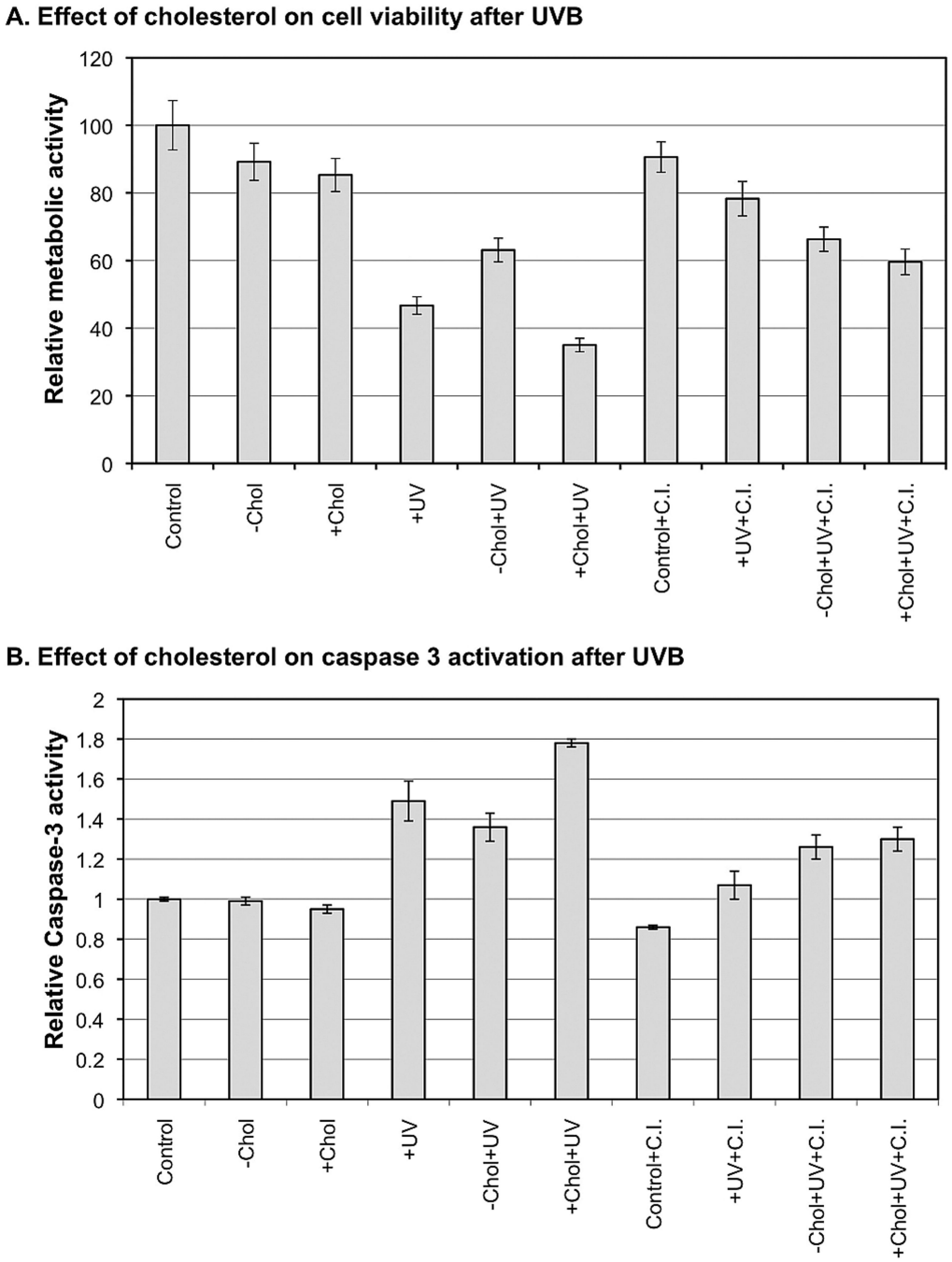

Figure 2.

The effect of cholesterol on cell viability and caspase 3 activation after UVB in M624 cells. Alamar Blue Assay was used to determine the viability of cells that had been UVB-irradiated, cholesterol-depleted and cholesterol-enriched. Caspase 3 activity was determined using a fluorometric assay method. The relative cell viabilities and caspase 3 activaiton were standardized to the viability of control cells. The data represents three sets of independent measurements.

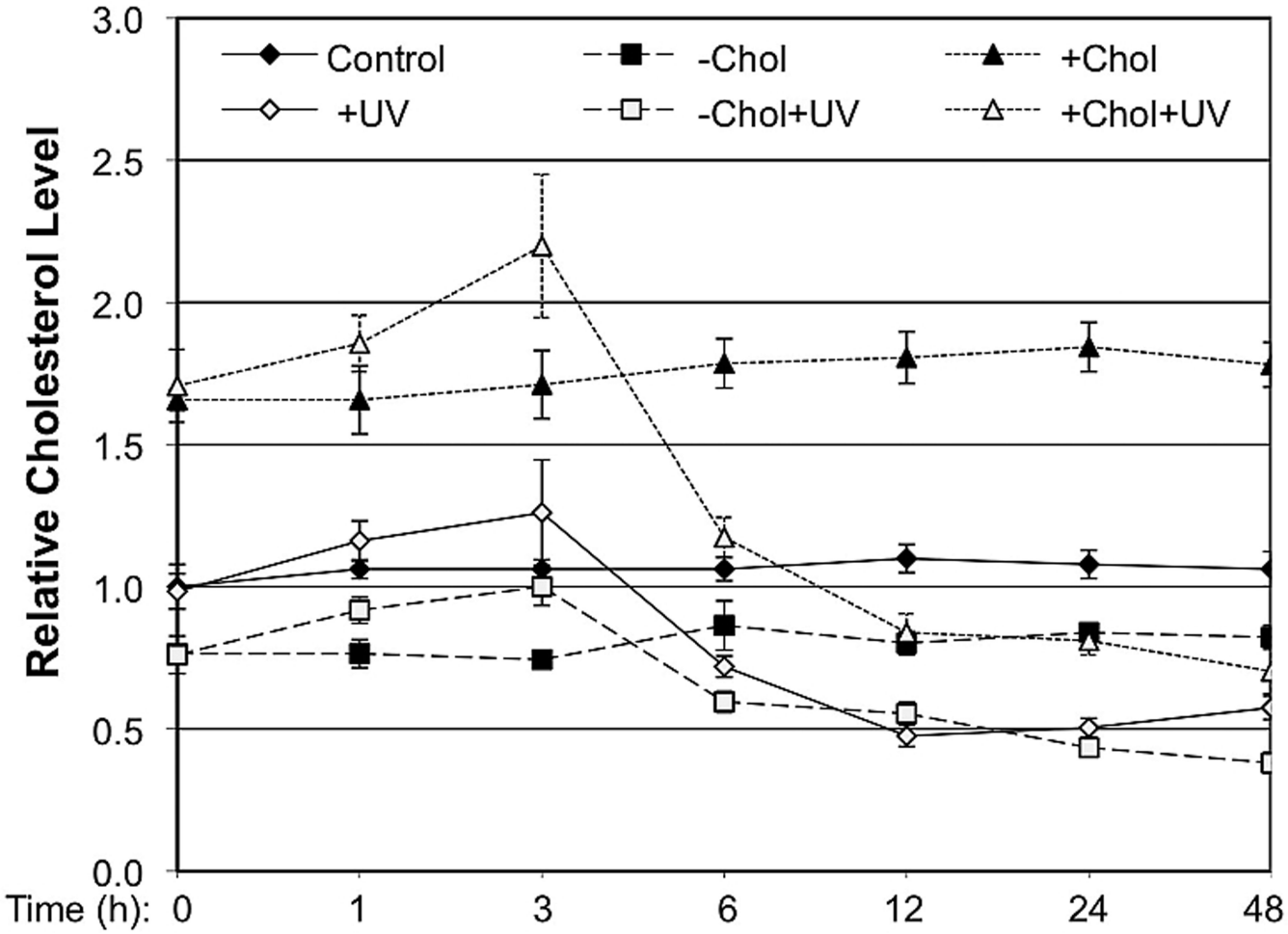

Figure 3.

The effects of UVB on cellular cholesterol levels of M624 cells. Total cholesterol in whole cell lysates of UVB-irradiated, cholesterol-enriched and cholesterol-depleted M624 cells was measured using Wako Cholesterol E kit. Relative cholesterol levels were standardized to the cholesterol level in the control cells. Results represent the average of three sets of independent measurements.

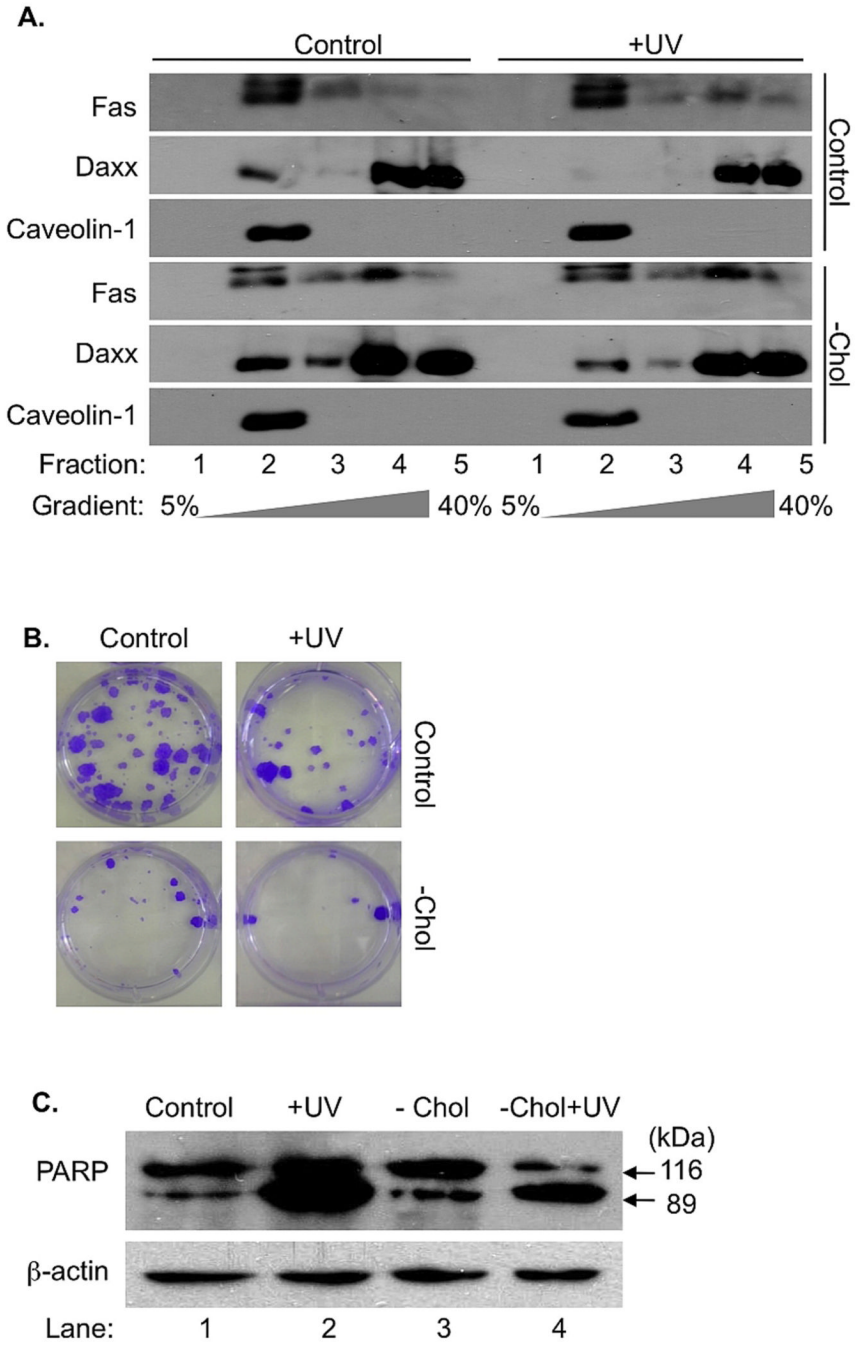

Figure 4.

The effects of UVB on Fas and Daxx distributions in gradient fractions, cell survival and apoptosis of cholesterol-depleted HaCaT cells. A: Total cell lysates were prepared from UVB-irradiated and cholesterol-depleted HaCaT cells and fractionated on an Optiprep gradient (40-30-5%). Equal volumes of each gradient fraction were buffered and SDS-PAGE was performed. Proteins were electroblotted onto nitrocellulose membrane, the membrane was blocked, and the distributions of Fas, Daxx, and caveolin-1 were analyzed by immunoblot using the corresponding antibodies. Results are representative of three independent experiments. B: Clonogenic assay was performed on UVB-irradiated and cholesterol-depleted HaCaT cells. Results are representative of three independent assays. C:

Total cell lysates were prepared from UVB-irradiated and cholesterol-depleted HaCaT cells and samples containing equal amounts of protein were buffered and SDS-PAGE was performed. Proteins were electroblotted onto nitrocellulose membrane, the membrane was blocked, and β-actin levels, PARP expression and PARP cleavage were analyzed by immunoblot using the corresponding antibodies. Results are representative of three independent experiments.

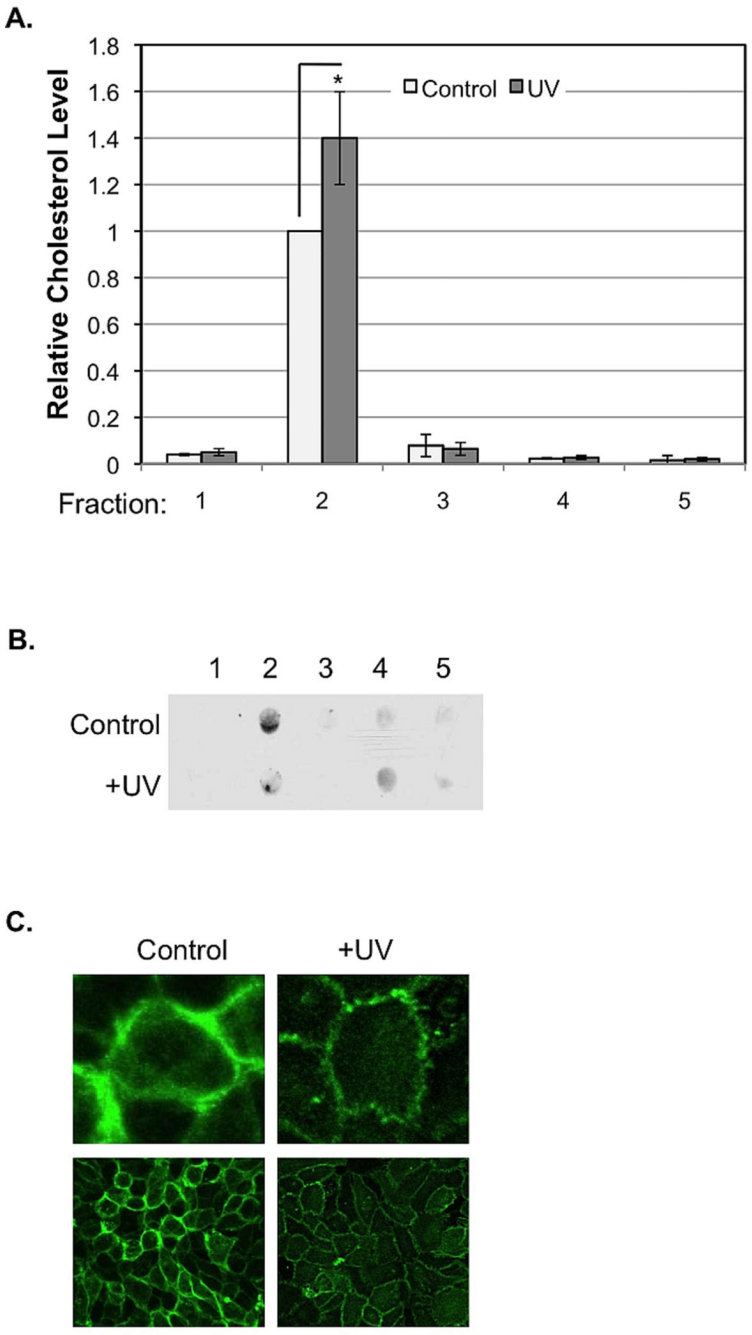

Figure 5.

The effects of UVB on raft cholesterol and ceramide levels and induced morphological changes. A: Total cholesterol in each fraction was measured using Wako Cholesterol E kit, and protein concentration of each fraction was measured using The Bradford Protein Assay Kit. Milligrams of cholesterol per gram of protein were calculated. Results represent the average of three sets of independent measurements (*: $p<0.05$). B: Ceramide levels in each fraction and whole cell lysate were examined by dot-blot analysis using an anti-ceramide antibody. Results are representative of three independent experiments. Relative ceramide levels were standardized to the ceramide level in the control cells (*: $p<0.05$ except for UVB/Chol-). C: Physical changes in UVB-irradiated HaCaT cells. Alexa Fluor 488-labeled

anti-GM1 was used to fluorescently label lipid rafts of UVB-irradiated HaCaT cells. The bottom images were captured with a Carl Zeiss fluorescence confocal microscope (LSM 510) with 40× lens. The top images were a computer magnification of a single cell from the bottom images.